

The Footprint of the CO₂ Plume during Carbon Dioxide Storage in Saline Aquifers: Storage Efficiency for Capillary Trapping at the Basin Scale

Ruben Juanes · Christopher W. MacMinn · Michael L. Szulczewski

Received: 23 December 2008 / Accepted: 14 May 2009 / Published online: 9 June 2009
© Springer Science+Business Media B.V. 2009

Abstract We study a sharp-interface mathematical model of CO₂ migration in deep saline aquifers, which accounts for gravity override, capillary trapping, natural groundwater flow, and the shape of the plume during the injection period. The model leads to a nonlinear advection–diffusion equation, where the diffusive term is due to buoyancy forces, not physical diffusion. For the case of interest in geological CO₂ storage, in which the mobility ratio is very unfavorable, the mathematical model can be simplified to a hyperbolic equation. We present a complete analytical solution to the hyperbolic model. The main outcome is a closed-form expression that predicts the ultimate footprint on the CO₂ plume, and the time scale required for complete trapping. The capillary trapping coefficient and the mobility ratio between CO₂ and brine emerge as the key parameters in the assessment of CO₂ storage in saline aquifers. Despite the many approximations, the model captures the essence of the flow dynamics and therefore reflects proper dependencies on the mobility ratio and the capillary trapping coefficient, which are basin-specific. The expressions derived here have applicability to capacity estimates by capillary trapping at the basin scale.

Keywords Geologic storage · Saline aquifers · Gravity currents · Capillary trapping · Residual trapping · Hysteresis · Sharp-interface · Storage efficiency · Capacity estimates

1 Introduction

Deep saline aquifers are attractive geological formations for the injection and long-term storage of CO₂ (IPCC 2005). Even if injected as a supercritical fluid—dense gas—the CO₂ is buoyant with respect to the formation brine. Several trapping mechanisms act to prevent the migration of the buoyant CO₂ back to the surface, and these include (IPCC 2005): (1) *structural and stratigraphic trapping*: the buoyant CO₂ is kept underground by an impermeable

R. Juanes (✉) · C. W. MacMinn · M. L. Szulczewski
Department of Civil and Environmental Engineering, Massachusetts Institute of Technology,
77 Massachusetts Ave., Bldg. 48-319, Cambridge, MA 02139, USA
e-mail: juanes@mit.edu

cap rock, either in a closed, nonmigrating system (static trapping) or in an open system where the CO₂ migrates slowly (hydrodynamic trapping) (Bachu et al. 1994); (2) *capillary trapping*: disconnection of the CO₂ phase into an immobile (trapped) fraction (Flett et al. 2004; Mo et al. 2005; Kumar et al. 2005; Juanes et al. 2006); (3) *solution trapping*: dissolution of the CO₂ in the brine, possibly enhanced by gravity instabilities (Ennis-King and Paterson 2005; Riaz et al. 2006); and (4) *mineral trapping*: geochemical binding to the rock due to mineral precipitation (Gunter et al. 1997). Because the time scales associated with these mechanisms are believed to be quite different ($t_{\text{struct}} \sim t_{\text{capil}} \ll t_{\text{dissol}} \ll t_{\text{miner}}$), it is justified to neglect dissolution and mineral trapping in the study of CO₂ migration during the injection and early post-injection periods—precisely when the risk for leakage is higher. Neglecting dissolution during the late post-injection period, however, is an assumption that warrants further study.

During the injection of CO₂ in the geologic formation, the gas saturation increases. Once the injection stops, the CO₂ continues to migrate in response to buoyancy and regional groundwater flow. At the leading edge of the CO₂ plume, gas continues to displace water in a drainage process (increasing gas saturation), while at the trailing edge water displaces gas in an imbibition process (increasing water saturations). The presence of an imbibition saturation path leads to snap-off at the pore scale and, subsequently, trapping of the gas phase. A trail of residual, immobile CO₂ is left behind the plume as it migrates along the top of the formation (Juanes et al. 2006).

The important questions that we address in this paper are: how far will the CO₂ plume travel (that is, what is the footprint of the plume), and for how long does the CO₂ remain mobile? An answer to these questions is essential in any first-order evaluation of the risk of a CO₂ storage project, and for obtaining capacity estimates at the basin scale.

In this paper, we develop a sharp-interface model of CO₂ injection and migration subject to background groundwater flow and capillary trapping. The model is one-dimensional, but captures the gravity override due to the density and mobility contrast between CO₂ and brine. When the mobility contrast is sufficiently high (as it is in the case of interest), we find, by solving the full problem numerically, that the model can be simplified to a hyperbolic equation.

We find a complete analytical solution to the hyperbolic model. This gives a closed-form expression for the footprint of the plume, and the associated time scale for complete immobilization of CO₂ by residual trapping. A capillary trapping coefficient Γ and the mobility ratio between brine and CO₂, M , emerge as the key parameters governing the footprint of the CO₂ plume. These analytical results can be used to estimate the efficiency factor for capillary trapping at the basin scale.

2 Description of the Physical Model

A schematic of the basin-scale geologic setting for which the flow model is developed is shown in Fig. 1. The CO₂ is injected in a deep formation (dark blue) that has natural groundwater flow (West to East in the diagram). The injection wells (red) are placed forming a line-drive pattern. The distance between wells is of the order of hundreds of meters to a kilometer. Therefore, the CO₂ plumes from the individual wells will interact early on in the life of the project. Under these conditions, the flow does not have large variations in the North–South direction. This simplification justifies the one-dimensional flow model developed here. The conceptual line-drive model is clearly an approximation, but a useful one. It provides a geologic context for one-dimensional gravity-current models of CO₂ migration (Vella and Huppert 2006; Hesse et al. 2007, 2008; Juanes and MacMinn 2008).

Fig. 1 Schematic of the basin-scale model of CO₂ injection. The CO₂ is injected in a deep formation (blue) that has a natural groundwater flow (West to East in the diagram). The injection wells (red) are placed forming a linear pattern in the deepest section of the aquifer. Under these conditions, the North–South component of the flow is negligible, and is not accounted for in the one-dimensional flow model developed here

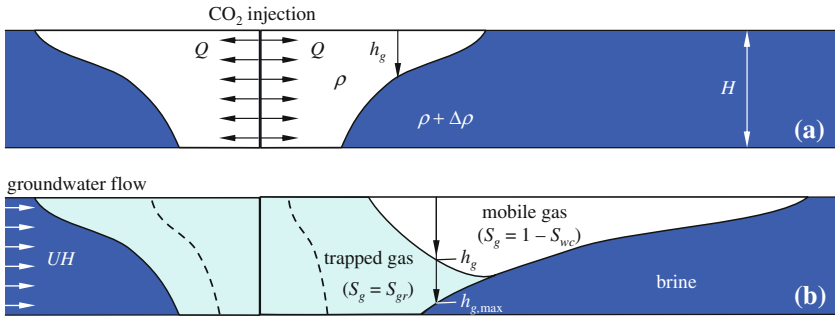
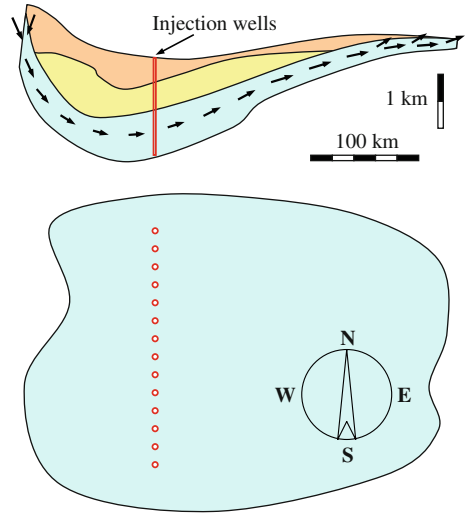


Fig. 2 Conceptual representation of the two different periods of CO₂ migration in a horizontal aquifer: **a** injection period and **b** post-injection period (see text for a detailed explanation)

We divide the study of the migration of CO₂ into two periods, shown in Fig. 2:

1. *Injection period.* Carbon dioxide (white) is injected at a high flow rate, displacing the brine (deep blue) to its irreducible saturation. Due to buoyancy, the injected CO₂ forms a gravity tongue.
2. *Post-injection period.* Once injection stops, the CO₂ plume continues to migrate due to its buoyancy and the background hydraulic gradient. At the trailing edge of the plume, CO₂ is trapped in residual form (light blue). The plume continues to migrate laterally, progressively decreasing its thickness until all the CO₂ is trapped.

Sharp-interface models of gravity currents in porous media have been studied for a long time (see, e.g., Barenblatt (1996) and Huppert and Woods (1995)). Analytical solutions for the evolution of an axisymmetric gravity current have been presented by Kochina et al. (1983), Lyle et al. (2005), and Nordbotten et al. (2005) (this last work in the context of CO₂ leakage through abandoned wells). Early-time and late-time similarity solutions for 1D gravity currents in horizontal aquifers are presented by Hesse et al. (2007). Of particular relevance is the work by Hesse et al. (2006): they developed a one-dimensional model that includes

capillary trapping and aquifer slope (which leads to an advection term). They solved their model numerically and used a “unit square” as the initial shape of the plume after injection.

Recently, analytical solutions to the hyperbolic limit of sharp-interface models of gravity currents with capillary trapping have been presented by Hesse et al. (2008) and Juanes and MacMinn (2008). Hesse et al. study a physical model with aquifer slope. They report a closed-form solution for the migration distance for the case of unit mobility ratio (in the context of CO₂ storage, however, the mobility of CO₂ is at least an order of magnitude larger than that of brine). In the general case, they employ numerical integration of the resulting ordinary differential equation. Juanes and MacMinn (2008) study a horizontal aquifer with regional groundwater flow, and use the analytical results to upscale capillary trapping to the aquifer scale.

In the next section, we extend our previous work (Juanes and MacMinn 2008) and present a sharp-interface mathematical model for the conceptual model of Fig. 2. Some of the distinctive features of our model are:

1. We model the *injection period*. We show that the shape of the plume at the end of injection leads to exacerbated gravity override, which affects the subsequent migration of the plume in a fundamental way.
2. We include the effect of *regional groundwater flow*, which is essential in the evolution of the plume after injection stops. Mathematically, the effect of a background flow is similar to that of nonzero aquifer slope—they both lead to a nonlinear advection term.
3. We obtain a simple *closed-form* analytical solution for all values of the mobility ratio.

3 Mathematical Model

We adopt a sharp-interface approximation (Huppert and Woods 1995), by which the medium is assumed to either be filled with water (water saturation $S_w = 1$) or filled with CO₂ (“gas” saturation $S_g = 1 - S_{wc}$, where S_{wc} is the irreducible connate water saturation). We assume that the dimension of the aquifer is much larger horizontally than vertically, so that the vertical flow equilibrium approximation (Bear 1972; Yortsos 1995) is applicable. This assumption dictates that flow is essentially horizontal, and the pressure variation in the vertical direction is hydrostatic. The aquifer is assumed to be horizontal and homogeneous. The fluid densities and viscosities are taken as constant. Indeed, compressibility and thermal expansion effects counteract each other, leading to a fairly constant supercritical CO₂ density over a significant range of depths (Bachu 2003). We also assume that dissolution into brine and leakage through the caprock are neglected. These assumptions are reviewed critically in the Discussion section.

Injection Period. Consider the encroachment of the injected CO₂ plume into the aquifer, as shown in Fig. 2(a). The density of the CO₂, ρ , is lower than that of the brine, $\rho + \Delta\rho$. Let h_g be the thickness of the (mobile) CO₂ plume, and H the total thickness of the aquifer.

The horizontal volumetric flux of each fluid is calculated by the multiphase flow extension of Darcy’s law, which involves the relative permeability to water, k_{rw} , and gas, k_{rg} (Bear 1972). In the mobile plume region, $k_{rw} = 0$ and $k_{rg} = k_{rg}^* < 1$. In the region outside the plume, $k_{rw} = 1$ and $k_{rg} = 0$. The volumetric flow rate of CO₂ injected is $Q = Q_{\text{well}} \frac{N_{\text{well}}}{W}$, where Q_{well} [L³T⁻¹] is the volumetric injection rate per well, N_{well} is the number of wells [–], and W is the width of the well array [L] (the dimensions of Q are L²T⁻¹, reflecting that the model collapses the third dimension of the problem). We assume that Q is much larger

than the vertically integrated natural groundwater flow. Since the formulation is similar to that of other works (Huppert and Woods 1995; Nordbotten et al. 2005; Hesse et al. 2008), we omit the derivation; details can be found in Juanes and MacMinn (2008). The governing equation for the plume thickness during injection reads

$$\phi(1 - S_{wc})\partial_t h_g + \partial_x(fQ - k\Delta\rho g H \bar{\lambda}_g(1 - f)\partial_x h_g) = 0, \tag{1}$$

where ϕ is the aquifer porosity, k is the permeability of the medium, g is the gravitational acceleration, $\bar{\lambda}_g = (k_{rg}^* h_g)/(\mu_g H)$ is the vertically averaged mobility of the CO₂, and f is the fractional flow of gas:

$$f = \frac{h_g}{h_g + \frac{\mu_g}{k_{rg}^* \mu_w} (H - h_g)}, \tag{2}$$

where μ_g and μ_w are the dynamic viscosities of gas and water, respectively.

Post-injection Period. Carbon dioxide is present in the mobile plume (with saturation $S_g = 1 - S_{wc}$) and as a trapped phase (with residual gas saturation $S_g = S_{gr}$). The governing equation for the plume thickness during the post-injection period is (Juanes and MacMinn 2008):

$$\phi R \partial_t h_g + \partial_x(fUH - k\Delta\rho g H \bar{\lambda}_g(1 - f)\partial_x h_g) = 0, \tag{3}$$

where U is the groundwater Darcy velocity and R is the accumulation coefficient:

$$R = \begin{cases} 1 - S_{wc} & \text{if } \partial_t h_g > 0 \text{ (drainage),} \\ 1 - S_{wc} - S_{gr} & \text{if } \partial_t h_g < 0 \text{ (imbibition).} \end{cases} \tag{4}$$

This equation is almost identical to Eq. 1 with two notable differences: (1) the coefficient in the accumulation term is discontinuous and (2) the advection term scales with the integrated groundwater flux, UH , and not the injected CO₂ flow rate, Q .

Dimensionless Form of the Equations. We define the dimensionless variables

$$h = \frac{h_g}{H}, \quad \tau = \frac{t}{T}, \quad \xi = \frac{x}{L}, \tag{5}$$

where T is the injection time and $L = QT/H\phi$ is a characteristic injection distance.

During injection, the plume evolution equation is

$$(1 - S_{wc})\partial_\tau h + \partial_\xi \left(f - N_g \frac{UH}{Q} h(1 - f)\partial_\xi h \right) = 0. \tag{6}$$

The behavior of the system is governed by the following two dimensionless parameters:

$$M = \frac{1/\mu_w}{k_{rg}^*/\mu_g} = \text{mobility ratio}, \tag{7}$$

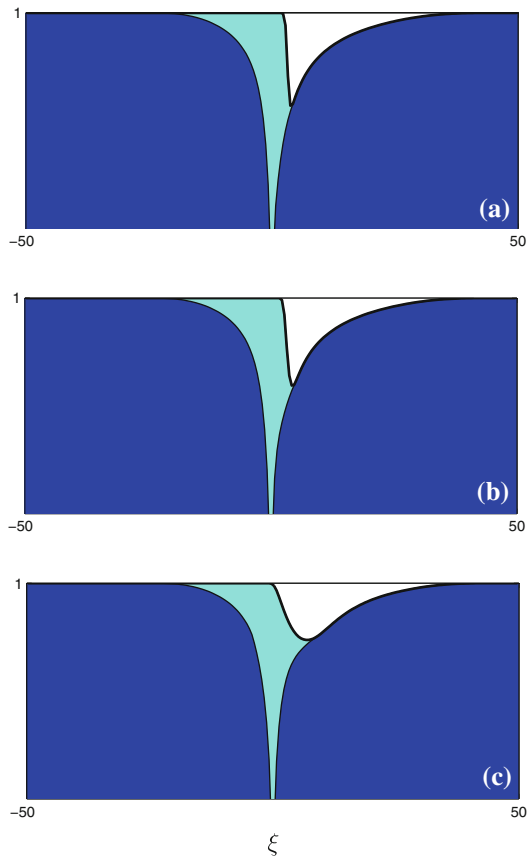
$$N_g = \frac{kk_{rg}^* \Delta\rho g}{\mu_g U} \frac{H}{(QT)/(H\phi)} = \text{gravity number}. \tag{8}$$

Equation 6 is a nonlinear advection–diffusion equation, where the second-order term comes from buoyancy forces, not physical diffusion.

During the post-injection period we re-scale time differently, to scale out the coefficient UH from the advection term. We choose, for $t > T$,

$$\tau = 1 + \frac{UH}{Q} \frac{t - T}{T}. \tag{9}$$

Fig. 3 Numerical solution to the full nonlinear advection–diffusion model. Shown are the profiles of the mobile CO₂ plume (*white*) and trapped CO₂ (*light blue*) at dimensionless time $\tau = 2$, for different values of the gravity number: **a** $N_g = 1$, **b** $N_g = 10$, **c** $N_g = 100$



The scaling in space remains unchanged. The governing equation during the post-injection period is

$$R\partial_\tau h + \partial_\xi(f - N_g h(1 - f))\partial_\xi h = 0. \quad (10)$$

The buoyancy term reflects the difference in time scaling.

4 Analytical Solution to the Hyperbolic Model

Equations 6 and 10 can be solved using standard discretization methods. Equation 6 is solved first to determine the evolution of the plume during injection. The shape at the end of injection is the initial condition for the post-injection period, governed by Eq. 10. In Fig. 3 we plot the numerical solution to the full advection–diffusion problem at a time well after injection stops. We used a typical value of the mobility ratio ($M = 0.1$), and values of the gravity number spanning several orders of magnitude. During the injection period, the effective gravity number is $N'_g = N_g \cdot UH/Q$. In our model, we assume that injection flow rates are much larger than natural groundwater fluxes ($Q \gg UH$). As a result, the influence of the buoyancy-diffusion term is much smaller during injection than during post-injection.

The simulations show that the footprint of the plume is almost insensitive to the value of the gravity number up to a value $N_g > 100$. These simulations justify dropping the second-order diffusive term from the formulation for a large range of gravity numbers. It is interesting (but not surprising) that for $M \ll 1$ the solution becomes independent of the density difference between the fluids, even though it is buoyancy that sets the gravity tongue.

The case $U = 0$ (that is, $N_g = \infty$) is obviously not covered by the hyperbolic model. Numerical solutions and late-time scaling laws for this case are presented by Hesse et al. (2006, 2008). In practice, either natural groundwater flow or aquifer slope will make the gravity number finite. The solution is then approximated by the hyperbolic model

$$R\partial_\tau h + \partial_\xi f = 0. \tag{11}$$

The complete analytical solution, obtained by the method of characteristics, is shown in Fig. 4. The top four figures show the profile of the plume at each stage of the CO₂ migration process: (a) injection, (b) retreat, (c) chase, and (d) sweep. The bottom figure (e) shows the solution on the dimensionless (ξ, τ) characteristic space.

Injection Period. During injection ($0 < \tau < 1$), we assume (see Fig. 2) that the solution is symmetric with respect to the injection well array. This means that we neglect the impact of the groundwater flow on the solution during the injection period. Therefore, only the displacement on the right half of the real line, $\xi > 0$, needs to be computed. The problem to be solved is a Riemann problem (Lax 1957; Smoller 1994), that is, the evolution of an initial discontinuity at $\xi = 0$:

$$h(\xi, \tau = 0) = \begin{cases} 1 & \xi \leq 0, \\ 0 & \xi > 0. \end{cases} \tag{12}$$

Since both the partial differential equation and the initial condition are invariant to a stretching of coordinates $(\xi, \tau) \mapsto (c\xi, c\tau)$ with $c > 0$, the solution can be expressed as a function of the characteristic velocity ζ :

$$h(\xi, \tau) = U(\zeta), \quad \zeta = \xi/\tau. \tag{13}$$

Since the flux function $f = h/(h + M(1 - h))$ is concave, the solution to the Riemann problem is a rarefaction wave, that is, a continuous solution that satisfies

$$U'(\zeta) = \frac{dU}{d\zeta} = \frac{1}{1 - S_{wc}} f'(U). \tag{14}$$

Therefore, the solution during injection is a simple rarefaction fan that evolves in both directions (Fig. 4(e)). The solution profile at the end of injection ($\tau_1 = 1$) is shown in Fig. 4(a), and the extent of the plume is

$$\xi_{inj} = \frac{1}{(1 - S_{wc})M}. \tag{15}$$

Retreat Stage. After injection stops ($\tau > 1$), the plume migrates to the right, subject to groundwater flow. The solution for the right side of the plume (drainage front) continues to be a divergent rarefaction fan. The solution for the left side of the plume (imbibition front), however, is now a convergent fan. Each state h travels with a characteristic speed that is faster than that of drainage, because residual CO₂ is being left behind. We define the *capillary trapping coefficient*

$$\Gamma = \frac{S_{gr}}{1 - S_{wc}} \quad (\text{always } \in [0, 1]). \tag{16}$$

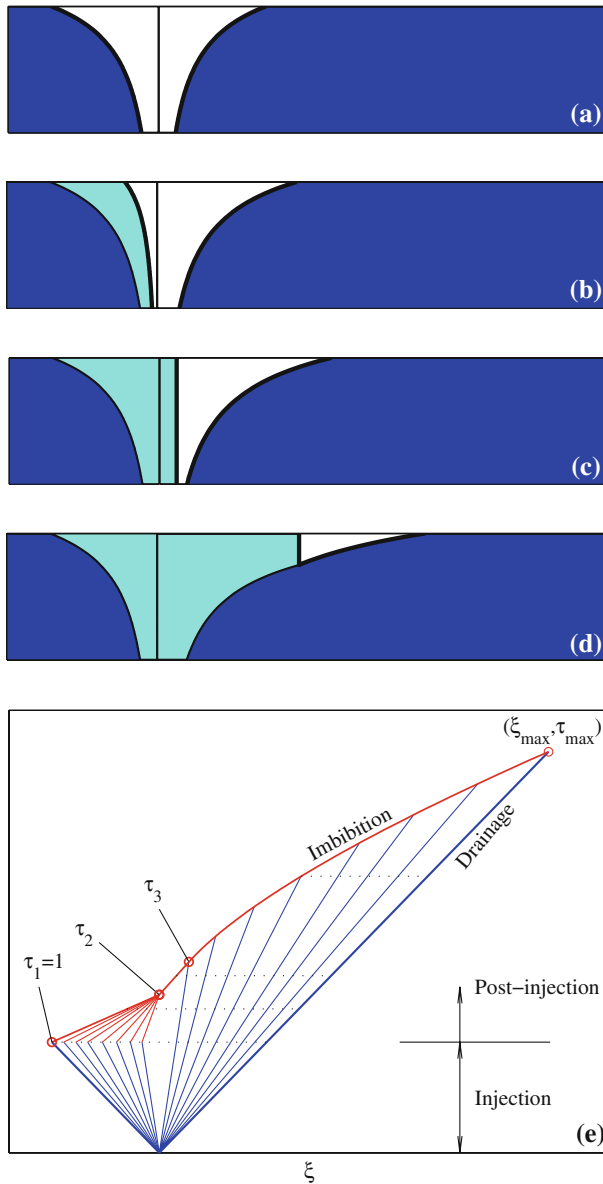


Fig. 4 Analytical solution to the hyperbolic model. Profiles of the mobile CO₂ plume (*white*) and trapped CO₂ (*light blue*) during the **a** injection period, **b** retreat stage, **c** chase stage, and **d** sweep stage. **e** Complete solution on (ξ, τ) -space until the entire CO₂ plume has been immobilized in residual form (see text for a detailed explanation)

At time $\tau_2 = 2 - \Gamma$, all characteristics impinge onto each other precisely at $\xi = 0$. Physically, this is the time at which the imbibition front becomes a discontinuity. The solution profile at a time $\tau < \tau_2$ is shown in Fig. 4(b).

Chase Stage. After the imbibition front passes through $\xi = 0$, due to the concavity of the flux function, the imbibition front is a genuine shock, that is, a traveling discontinuity that propagates at a speed given by the Rankine–Hugoniot condition (Smoller 1994):

$$\sigma = \frac{1}{1 - S_{wc} - S_{gr}}. \tag{17}$$

While the imbibition shock advances, the continuous drainage front continues to propagate exactly as before. The solution during this stage is shown in Fig. 4(c). This period ends at time $\tau_3 = (2 - \Gamma)/(1 - M(1 - \Gamma))$, when the imbibition shock wave (thick red line) collides with the slowest ray of the drainage rarefaction wave (thin blue line) in Fig. 4(e). Physically, this is the time at which the CO₂ plume detaches from the bottom of the aquifer.

Sweep Stage. Once the mobile plume detaches from the bottom of the aquifer, the solution comprises the continuous interaction of a progressively faster shock with a rarefaction wave. The problem is solved if one determines the evolution of the plume thickness at the imbibition front, h_m , as a function of dimensionless time τ . The differential equation governing the evolution of the state h_m can be obtained by finding the intersection (on the (ξ, τ) -space) of the imbibition shock wave corresponding to a state h_m with the rarefaction ray for a state $h_m + dh_m$, and taking the limit $dh_m \rightarrow 0$. The resulting differential equation is:

$$\left(\frac{1}{1 - S_{wc} - S_{gr}} \frac{f(h_m)}{h_m} - \frac{1}{1 - S_{wc}} f'(h_m) \right) d\tau = \frac{1}{1 - S_{wc}} f''(h_m) \tau dh_m. \tag{18}$$

The initial condition is $h_m = 1$ at $\tau = \tau_3$. After separation of variables, Eq. 18 can be written as follows:

$$\int_{\tau_3}^{\tau} \frac{d\tau}{\tau} = \int_1^{h_m} \frac{f''(h)}{\frac{1}{1-\Gamma} \frac{f(h)}{h} - f'(h)} dh. \tag{19}$$

The integral in Eq. 19 can be evaluated analytically, and the solution admits a closed-form expression:

$$\tau(h_m) = (2 - \Gamma)(1 - M(1 - \Gamma)) \left(\frac{M + (1 - M)h_m}{M\Gamma + (1 - M)h_m} \right)^2. \tag{20}$$

In Fig. 4(d), we plot the profile of the CO₂ plume at some time during the sweep stage. A representation of the solution in characteristic space is shown in Fig. 4(e). The thick red line corresponds to the imbibition front. When the imbibition front collides with the fastest ray, the entire CO₂ plume is in residual, immobile form. This occurs at a dimensionless time $\tau_{\max} = \tau(h_m = 0)$.

5 Footprint of the CO₂ Plume and Trapping Efficiency Factor

An important practical result from the analytical solution derived above is a closed-form expression for the time scale for complete trapping,

$$\tau_{\max} = \frac{(2 - \Gamma)(1 - M(1 - \Gamma))}{\Gamma^2}. \tag{21}$$

and the maximum migration distance of the CO₂ plume,

$$\xi_{\max} = \frac{(2 - \Gamma)(1 - M(1 - \Gamma))}{\Gamma^2} \frac{1}{(1 - S_{wc})M}. \tag{22}$$

The corresponding dimensional quantities (time for trapping t_{\max} and maximum trapping length x_{\max}) can be obtained simply by multiplying by the injection period T and the characteristic injection distance L , respectively.

The mobility ratio M (Eq. 7) and the capillary trapping coefficient Γ (Eq. 16) emerge as the key parameters in the assessment of CO₂ storage in saline aquifers. The capillary trapping coefficient is always between zero and one, and it increases with increasing residual gas saturation. Larger values of Γ result in more effective trapping of the CO₂ plume. It is not surprising that the ultimate footprint of the plume is inversely proportional to the mobility ratio M . The maximum migration distance is also strongly dependent on the shape of the plume at the end of the injection period, suggesting that it is essential to model the injection period for proper assessment of the ultimate footprint of the plume—this is in agreement with the findings for the case of a spreading plume without groundwater flow (MacMinn and Juanes 2008b).

Our model also permits the determination of the storage capacity of a geologic basin, and the *storage efficiency factor due to capillary trapping*. Defining the efficiency factor as the ratio of the volume of CO₂ injected and the pore volume of the aquifer $V_{\text{CO}_2} = E_{\text{capil}} V_{\text{pore}}$ (Bachu et al. 2007), it takes the following simple expression:

$$E_{\text{capil}} = \frac{2}{\xi_{\text{inj}} + \xi_{\text{max}}} = 2(1 - S_{wc})M \frac{\Gamma^2}{\Gamma^2 + (2 - \Gamma)(1 - M(1 - \Gamma))}. \tag{23}$$

This simple algebraic expression can be used to evaluate quickly the footprint that can be expected from a CO₂ sequestration project at the basin scale. Consider an aquifer with $k = 100 \text{ md} = 10^{-13} \text{ m}^2$, $\phi = 0.2$, and $H = 100 \text{ m}$. Injection conditions are about 100 bar and 40 °C. Under these conditions, $\rho \approx 400 \text{ kg m}^{-3}$, $\Delta\rho \approx 600 \text{ kg m}^{-3}$, $\mu_g \approx 0.05 \times 10^{-3} \text{ kg m}^{-1} \text{ s}^{-1}$, and $\mu_w \approx 0.8 \times 10^{-3} \text{ kg m}^{-1} \text{ s}^{-1}$. We take the following rock–fluid property values: $S_{wc} = 0.4$, $S_{gr} = 0.3$, and $k_{rg}^* = 0.6$ (Bennion and Bachu 2006). These parameters lead to the following values of the trapping coefficient and the mobility ratio: $\Gamma = 0.5$ and $M \approx 0.1$. Consider a major sequestration project, in which 100 megatonnes of CO₂ are injected every year, for a period of $T = 50$ years—a realistic time span of the sequestration effort. This scenario corresponds to the injection of the CO₂ emitted by about 20 medium-size coal-fired power plants. The injection rate is of the same order as (but less than) the yearly CO₂ emissions from coal-fired power plants in several states in the US (Texas, Indiana, Ohio, and Pennsylvania each emit $\sim 150 \text{ MtCO}_2/\text{year}$ from coal alone (Energy Information Administration 2008)). In fact, similar scenarios (line drive of wells with a total injection rate of 50–250 MtCO₂/year for 50 years) have been the subject of recent assessments for the Texas Gulf Coast aquifer system (Nicot 2008). If injection takes place at 100 wells, with interwell spacing of 1 km, then $Q = 1250 \text{ m}^2 \text{ yr}^{-1}$ and $Q/H = 12.5 \text{ m yr}^{-1}$. Assume that the background groundwater flow is $U = 0.1 \text{ m yr}^{-1}$. The corresponding gravity number is $N_g \approx 120$, still within the range of validity of the hyperbolic approximation. For this set of parameters, the expected footprint of the plume and time scale for complete trapping are (in dimensionless quantities):

$$\xi_{\max} = 95, \quad \tau_{\max} = 5.7.$$

It is instructive to convert them to dimensional values:

$$x_{\max} = \frac{QT}{H\phi} \xi_{\max} \approx 300 \text{ km},$$

$$t_{\max} = T \left(1 + \frac{Q}{UH} \right) (\tau_{\max} - 1) \approx 30,000 \text{ years}.$$

The corresponding value of the capillary trapping efficiency factor is $E_{\text{capil}} \approx 1.8\%$ which, in this particular case, is in the range of 1–4% suggested by the DOE Regional Carbon Sequestration Partnerships (Bachu et al. 2007; Department of Energy 2007).

6 Discussion and Conclusions

The results above suggest that it is the scale of hundreds of kilometers in space, and thousands of years in time, that is relevant for the assessment of geological CO₂ sequestration at the gigatonne scale.

The applicability of the model hinges on some important assumptions and approximations. Aquifer heterogeneity, for example, will often increase the migration distance. The gravity tongue, however, is a persistent feature of the flow that is likely to dominate the picture, regardless of heterogeneity. The model assumes a sharp interface approximation. In reality, due to the finite size of the transition region between the CO₂ plume and the formation brine, the plume may become immobile before it reaches zero thickness—from this point of view, our estimates are on the safe side.

The caprock of aquifers will often have undulations. This will lead to additional *stratigraphic* trapping, resulting in smaller migration distances. We expect, however, that the estimates of *capillary* trapping will not be largely affected by this effect, since the CO₂ that is trapped in local anticlines is not subject to imbibition process and remains mobile.

Due to the large time scales expected, the assumption of neglecting dissolution of CO₂ in the brine becomes questionable. We are currently developing analytical models that incorporate the effect of CO₂ dissolution (MacMinn and Juanes 2008a). Dissolution will decrease the migration distance. One way to accelerate the time to trap the CO₂ (and make the no dissolution and hyperbolic approximations more applicable) is to inject water slugs, along with the CO₂ (Juanes et al. 2006).

The model also neglects loss of CO₂ through the caprock. Application of the analytical solution requires that geological features that serve as conduits for vertical fluid migration be mapped, and that the well array of Fig. 1 be placed such that the plume avoids such features (which include outcrops, faults, conductive fractures, etc.)

Despite the many approximations, the model captures the essence of the flow dynamics and therefore reflects proper dependencies on the mobility ratio and the capillary trapping coefficient, which are basin-specific. The analytic expressions derived here can be used for capacity assessment of capillary trapping at the basin scale (Szulczewski and Juanes 2009).

Acknowledgements Funding for this work was provided by a Reed Research Grant, the MIT Energy Initiative, and the ARCO Chair in Energy Studies. This funding is gratefully acknowledged.

References

- Bachu, S.: Screening and ranking of sedimentary basins for sequestration of CO₂ in geological media in response to climate change. *Environ. Geol.* **44**, 277–289 (2003)
- Bachu, S., Gunther, W.D., Perkins, E.H.: Aquifer disposal of CO₂: hydrodynamic and mineral trapping. *Energy Conv. Manag.* **35**(4), 269–279 (1994)
- Bachu, S. et al.: CO₂ storage capacity estimation: methodology and gaps. *Int. J. Greenhouse Gas Control* **1**, 430–443 (2007)
- Barenblatt, G.I.: *Scaling, Self-similarity, and Intermediate Asymptotics*. Cambridge Texts in Applied Mathematics, Cambridge University Press (1996)

- Bear, J.: Dynamics of fluids in porous media. Elsevier, New York, reprinted with corrections, Dover, New York, 1988 (1972)
- Bennion, D.B., Bachu, S.: Supercritical CO₂ and H₂S—brine drainage and imbibition relative permeability relationships for intergranular sandstone and carbonate formations. In: SPE Europec/EAGE Annual Conference and Exhibition, Vienna, Austria (SPE 99326) (2006)
- Department of Energy NETL: Carbon Sequestration Atlas of the United States and Canada. (2007) http://www.netl.doe.gov/technologies/carbon_seq/refshelf/atlas/
- Energy Information Administration: State energy-related carbon dioxide emissions estimates (2008) http://www.eia.doe.gov/oiaf/1605/ggrpt/excel/tbl_statefuel.xls
- Ennis-King, J., Paterson, L.: Role of convective mixing in the long-term storage of carbon dioxide in deep saline formations. *Soc. Pet. Eng. J.* **10**(3), 349–356 (2005)
- Flett, M., Gurton, R., Taggart, I.: The function of gas–water relative permeability hysteresis in the sequestration of carbon dioxide in saline formations. In: SPE Asia Pacific Oil and Gas Conference and Exhibition, Perth, Australia (SPE 88485) (2004)
- Gunter, W.D., Wiwchar, B., Perkins, E.H.: Aquifer disposal of CO₂-rich greenhouse gases: Extension of the time scale of experiment for CO₂-sequestering reactions by geochemical modeling. *Miner. Pet* **59**(1–2), 121–140 (1997)
- Hesse, M.A., Tchelepi, H.A., Orr, F.M. Jr.: Scaling analysis of the migration of CO₂ in saline aquifers. In: SPE Annual Technical Conference and Exhibition, San Antonio, TX (SPE 102796) (2006)
- Hesse, M.A., Tchelepi, H.A., Cantwel, B.J., Orr, F.M. Jr.: Gravity currents in horizontal porous layers: transition from early to late self-similarity. *J. Fluid Mech.* **577**, 363–383 (2007)
- Hesse, M.A., Orr, F.M. Jr., Tchelepi, H.A.: Gravity currents with residual trapping. *J. Fluid Mech.* **611**, 35–60 (2008)
- Huppert, H.E., Woods, A.W.: Gravity-driven flows in porous media. *J. Fluid Mech.* **292**, 55–69 (1995)
- IPCC: Special report on carbon dioxide capture and storage. In: Metz, B., et al. (eds.) Cambridge University Press (2005)
- Juanes, R., MacMinn, C.W.: Upscaling of capillary trapping under gravity override: application to CO₂ sequestration in aquifers. In: SPE/DOE Symposium on Improved Oil Recovery, Tulsa, OK (SPE 113496) (2008)
- Juanes, R., Spiteri, E.J., Orr, F.M. Jr., Blunt, M.J.: Impact of relative permeability hysteresis on geological CO₂ storage. *Water Resour. Res.* **42**, W12418 (2006). doi:[10.1029/2005WR004806](https://doi.org/10.1029/2005WR004806)
- Kochina, I.N., Mikhailov, N.N., Filinov, M.V.: Groundwater mound damping. *Int. J. Eng. Sci.* **21**, 413–421 (1983)
- Kumar, A., Ozah, R., Noh, M., Pope, G.A., Bryant, S., Sepehrnoori, K., Lake, L.W.: Reservoir simulation of CO₂ storage in deep saline aquifers. *Soc. Pet. Eng. J.* **10**(3), 336–348 (2005)
- Lax, P.D.: Hyperbolic systems of conservation laws, II. *Comm. Pure Appl. Math.* **10**, 537–566 (1957)
- Lyle, S., Huppert, H.E., Hallworth, M., Bickle, M., Chadwick, A.: Axisymmetric gravity currents in a porous medium. *J. Fluid Mech.* **543**, 293–302 (2005)
- MacMinn, C.W., Juanes, R.: Integrating CO₂ dissolution into analytical models for geological CO₂ storage. In: 61st Annual Meeting of the APS Division of Fluid Dynamics, San Antonio, TX (2008a)
- MacMinn, C.W., Juanes, R.: Post-injection spreading and trapping of CO₂ in saline aquifers. *Comput. Geosci.* (Submitted) (2008b)
- Mo, S., Zweigel, P., Lindeberg, E., Akervoll, I.: Effect of geologic parameters on CO₂ storage in deep saline aquifers. In: 14th Europec Biennial Conference, Madrid, Spain (SPE 93952) (2005)
- Nicot, J.P.: Evaluation of large-scale CO₂ storage on fresh-water sections of aquifers: an example from the Texas Gulf Coast Basin. *Int. J. Greenhouse Gas Control* **2**(4), 582–593 (2008)
- Nordbotten, J.M., Celia, M.A., Bachu, S.: Analytical solution for CO₂ plume evolution during injection. *Transp. Porous Media* **58**(3), 339–360 (2005)
- Riaz, A., Hesse, M., Tchelepi, H.A., Orr, F.M. Jr.: Onset of convection in a gravitationally unstable, diffusive boundary layer in porous media. *J. Fluid Mech.* **548**, 87–111 (2006)
- Smoller, J.: Shock waves and reaction-diffusion equations. Springer-Verlag, New York (1994)
- Szulczewski, M.L., Juanes, R.: A simple but rigorous model for calculating CO₂ storage capacity in deep saline aquifers at the basin scale. *Energy Procedia (Proc GHGT-9)* **1**(1), 3307–3314 (2009) doi:[10.1016/j.egypro.2009.02.117](https://doi.org/10.1016/j.egypro.2009.02.117)
- Vella, D., Huppert, H.E.: Gravity currents in a porous medium at an inclined plane. *J. Fluid Mech.* **555**, 353–362 (2006)
- Yortsos, Y.C.: A theoretical analysis of vertical flow equilibrium. *Transp. Porous Media* **18**, 107–129 (1995)